Canadian Mineralogist
Vol. 17, pp. 757-769 (1979)

THE STABILITY OF LIZARDITE

LOUIS J. CARUSO* AND JOSEPH V. CHERNOSKY, JR.
Department of Geological Sciences, University of Maine at Orono, Orono, Maine 04473, U.S.A.

ABSTRACT

The dehydration reaction

$$10Mg_{5.5}Al_{1.0}Si_{3.5}O_{10}(OH)_8 = 2Mg_3Si_4O_{10}(OH)_2 + 12Mg_2SiO_4 + 5Mg_5Al_2Si_3O_{10}(OH)_8 + 18H_2O$$
(lizardite) (talc) (forsterite) (clinochlore) (fluid)

has been bracketed, with reversed experiments and $P(H_2O) = P_{total}$. A smooth curve drawn between the experimental brackets passes through the P–T coordinates 0.5 kbar, 540°C; 2 kbar, 582°C; 3 kbar, 591°C; 5 kbar, 602°C; 6 kbar, 606°C. Synthetic lizardite, clinochlore, talc and forsterite were used as starting materials. The standard entropy of formation (–2290 ± 86 J mol^{-1} deg^{-1}), the Gibbs free energy of formation (–8220 ± 48 kJ mol^{-1}) and the standard enthalpy of formation (8903 ± 54 kJ mol^{-1}) of lizardite at 298 K, 1 bar were calculated from the bracketing data for the reaction. The position of the reaction with respect to experimentally determined dehydration equilibria involving chrysotile and antigorite indicates that the thermal stability of lizardite increases with increasing aluminum content: the substitution of $2Al^{3+}$ for $Mg^{2+} + Si^{4+}$ decreases the lateral dimensions of the octahedral sheet and increases those of the tetrahedral sheet, thereby reducing the mismatch and the intralayer strain, and enhancing the thermal stability. A multisystem involving the phases lizardite, clinochlore, talc, brucite, antigorite, forsterite and water, constructed and refined in the system $MgO–Al_2O_3–SiO_2–H_2O$, indicates that aluminous lizardite may have a higher thermal stability than antigorite at low pressure. The pressure at which antigorite becomes thermally more stable than aluminous lizardite is governed by the compositions of both serpentines.

SOMMAIRE

La réaction de déshydratation

$$10Mg_{5.5}Al_{1.0}Si_{3.5}O_{10}(OH)_8 = 2Mg_3Si_4O_{10}(OH)_2 + 12Mg_2SiO_4 + 5Mg_5Al_2Si_3O_{10}(OH)_8 + 18H_2O$$
(lizardite) (talc) (forstérite) (clinochlore) (fluide)

a été encadrée, avec expériences renversées et $P(H_2O) = P_{total}$. La courbe tracée à l'intérieur des fourchettes expérimentales passe par les points dont les coordonnées P–T sont: 0.5 kbar, 540°C; 2 kbar, 582°C; 3 kbar, 591°C; 5 kbar, 602°C; 6 kbar, 606°C. Lizardite, clinochlore, talc et forstérite (synthétiques) étaient les produits de départ. Pour la lizardite à 298 K et 1 bar, l'entropie normale de formation (–2290 ± 86 J mol^{-1} deg^{-1}), l'énergie libre (Gibbs) de formation (–8220 ± 48 kJ mol^{-1}) et l'enthalpie normale de formation (8903 ± 54 kJ mol^{-1}) ont été calculées à partir des données de l'encadrement de la réaction. De la position de la réaction par rapport aux équilibres de déshydratation déterminés expérimentalement, on conclut que la stabilité de la lizardite s'accroît avec la teneur en aluminium: la substitution de $2Al^{3+}$ à $Mg^{2+} + Si^{4+}$ diminue les dimensions de la couche d'octaèdres et augmente celles de la couche des tétraèdres, donnant ainsi un meilleur appariement, qui réduit les tensions internes et améliore la stabilité thermique. Un multisystème comprenant les phases lizardite, clinochlore, talc, brucite, antigorite, forstérite et eau, construit et affiné dans le système $MgO–Al_2O_3–SiO_2–H_2O$, indique pour la lizardite aluminifère une stabilité thermique supérieure à celle de l'antigorite à basse pression. C'est la composition des deux serpentines qui détermine la pression à laquelle l'antigorite devient thermiquement plus stable que cette lizardite.

(Traduit par la Rédaction)

INTRODUCTION

Lizardite was recognized as a distinct mineral species by Whittaker & Zussman (1956), who found that it possesses a one-layer orthogonal unit-cell and flat layers rather than cylindrical layers as in chrysotile or corrugated layers as in antigorite. There is considerable ambiguity in the petrological literature regarding the nomenclature of the flat-layer serpentines; these have been called aluminous serpentine (Yoder 1952), septechlorite (Nelson & Roy 1958), *n*-layer serpentine (where *n* refers to the number of layers in the unit cell: Gillery 1959) and 7 Å chlorite. We have adopted the proposal (Wicks & Whittaker 1975) that flat-layer aluminous serpentines along the join $Mg_6Si_4O_{10}(OH)_8$ –

*Present address: Department of Earth and Planetary Sciences, Massachusetts Institute of Technology, Cambridge, Mass. 02139, U.S.A.

$Mg_4Al_4Si_2O_{10}(OH)_8$ be named lizardites in order that one-layer and multilayer serpentines can be considered polytypes. Although the structure of lizardite is approximately 1*T* (Rucklidge & Zussman 1965, Bailey 1969), we shall use the double formula $(Mg_{6-x}Al_x)(Si_{4-x}Al_x)O_{10}(OH)_8$ where x refers to the mole number of aluminum, in order to facilitate comparison with the earlier literature.

Lizardite is probably the most abundant serpentine mineral; it is readily synthesized in the laboratory, yet little is known about its stability and nothing is known about its thermochemical parameters. Yoder (1952) first synthesized lizardite with $x = 1.0$ and showed that it slowly converted to clinochlore at temperatures above about 520°C; attempts to reverse this reaction were unsuccessful. Similar results were obtained by Roy & Roy (1955). Nelson & Roy (1958) determined that lizardites with varying aluminum contents reacted to chlorite, talc and forsterite but did not reverse the reaction. Preliminary experimental work on the stability of lizardite with $x = 0.2$ (Chernosky 1973a) suggested that its stability increases with increasing aluminum content.

The stability of lizardite is a matter of current debate among petrologists. Evans (1977, p. 410) postulated that "lizardite probably occurs stably, if at all, only at very low temperatures" because "the chemically equivalent pair antigorite + chlorite occurs widely in thoroughly recrystallized serpentinites." Frost (1973), on the other hand, observed that aluminous lizardite ($\sim$ 5 wt. % Al_2O_3, $x \sim 0.27$) persisted in a contact aureole 30 metres beyond the antigorite-out isograd. He entertained the possibility that Al–lizardite is more stable than antigorite but later (Frost 1975) proposed that lizardite is metastable. Dungan (1979) observed aluminous lizardite containing about 5 wt. % Al_2O_3 in bastite pseudomorphs surrounded by radiating antigorite blades in a serpentinite subjected to the highest metamorphic grade to which antigorite is stable; he concluded that lizardite is metastable except perhaps at very low temperatures. This conclusion was based in part on the observation that lizardite persists in unsheared serpentinite but is absent from sheared serpentinite.

We have determined experimentally the high-temperature stability of an aluminous lizardite in an attempt to resolve conflicting opinions regarding its stability. The low-temperature stability of lizardite with respect to chrysotile- and antigorite-bearing assemblages was not determined experimentally. The purpose of this paper is to report our experimental results pertaining to the stability of lizardite containing 9.25 wt. % Al_2O_3 ($x = 0.5$). Our results confirm Chernosky's preliminary data and indicate that lizardite is stable to surprizingly high temperatures. We hope to demonstrate that the high thermal stability of lizardite is consistent with its structure.

The discussion will be limited to one-layer lizardites, which have only been synthesized from mixes with $x \leq 0.65$; mixes with higher aluminum contents yield six-layer rather than one-layer lizardites (Gillery 1959). The description of naturally occurring multilayer lizardites with aluminum contents ranging from 13.6 ($x = 0.74$) to 15.1 ($x = 0.82$) wt. % Al_2O_3 (Wicks & Plant 1979) supports the compositional limit for one-layer lizardite proposed by Gillery (1959).

Experimental Methods

Starting materials

Mixtures having bulk compositions $2MgO \cdot SiO_2$ and $3MgO \cdot 4SiO_2$ were prepared by drying, weighing and mixing appropriate proportions of MgO (Fisher, lot 787699) and SiO_2 glass (Corning lump cullet 7940, lot 62221). SiO_2 glass and MgO were fired at 1000°C for two hours to drive off adsorbed water. "Gels" having bulk compositions $5.5MgO \cdot 0.5Al_2O_3 \cdot 3.5SiO_2$ and $5MgO \cdot Al_2O_3 \cdot 3SiO_2$ were prepared by mixing the required weights of standardized nitrate solutions of magnesium and aluminum; tetraethyl orthosilicate (TEOS) was used as a source of silica. The coprecipitated gels were dried and then fired at 700–800°C to drive off nitrates. Forsterite, talc, clinochlore and lizardite were hydrothermally synthesized from the oxide mixes or gels. Purity and crystallinity of the synthetic phases were confirmed by examination with a petrographic microscope and X-ray diffraction.

Starting materials used to bracket the reaction were prepared by mixing synthetic lizardite with stoichiometric proportions of synthetic clinochlore, talc and forsterite and grinding for one-half hour to ensure homogeneity. Charges were prepared by sealing approximately 15 mg of starting material together with excess distilled, deionized water in 1.25-cm-long gold capsules.

Procedure

All experiments were conducted in horizontally mounted cold-seal hydrothermal vessels made of Haynes Alloy #25 (Stellite) or René 41.

Pressures were measured with factory-calibrated, sixteen-inch Heise gauges assumed accurate to ± 0.1% of full scale (0–4000 bars and 0–7000 bars). In order to conserve valve stems and packings, pressures were monitored carefully at the initiation of each experiment to guard against possible leaks and were then monitored on a weekly or biweekly basis. Minor fluctuations in pressure resulting from temperature drift did occur; however, experiments that suffered pressure drops of greater than 50 bars were discarded. Pressures are believed accurate to within ± 1 % of the stated value.

The temperature of each experiment was recorded daily. Errors in temperature are reported as ± 2 standard deviations about the mean temperature and represent error due solely to temperature drift. Error due to temperature gradients in the pressure vessels is assumed negligible, because temperature gradients were determined to be less than 1°C over a working distance of 3.0 cm (calibration performed at room pressure). The temperature calibration for each shielded thermocouple was checked after every experiment by heating the vessel to the temperature of the experiment at a pressure of 1 bar and comparing the measured temperature to that of a previously standardized thermocouple placed inside the vessel; corrections were on the order of 0–5°C. This procedure ensures internally consistent temperatures among experiments performed in different pressure vessels. All experiments were checked for leaks before and after hydrothermal treatment by heating the capsule for three minutes at 300°C and 1 bar and determining if a loss of water had occurred.

The experimental products were examined with a petrographic microscope and by X-ray powder diffraction. Owing to sluggish reaction rates at temperatures and pressures close to the phase boundary, complete reaction was never observed. Determination of reaction direction at a given temperature and pressure was based on a comparison of an X-ray pattern of an experimental product with an X-ray pattern of the starting material over the interval 5° to 65° 2θ (Cu $K\alpha$ radiation). Owing to overlap of numerous X-ray reflections, the following reflections were found most suitable for judging reaction direction: d_{201} and d_{060} of lizardite, d_{001} of clinochlore, d_{002} of talc and d_{112} of forsterite. A reaction was considered reversed if a 20% change in the intensities of X-ray reflections of an experimental product relative to those of the starting material could be observed. Microscopic observation of the experimental products did not reveal textural criteria that could be used to judge reaction direction.

Unit-cell parameters for synthetic phases used in the starting material were calculated by refining powder patterns obtained using the Enraf–Nonius FR552 Guinier camera and Cu $K\alpha$ radiation; CaF_2 (Baker Lot 91548, a = 5.4620 ± 0.0005) standardized against gem diamond (a = 3.56703, Robie *et al.* 1966) was used as an internal standard. Least-squares unit-cell refinements were performed using the computer program of Appleman & Evans (1973).

Results

Synthesis and characterization of phases

Lizardite $Mg_{5.5}Al_{0.5}Si_{3.5}Al_{0.5}O_{10}(OH)_{10}$ was synthesized hydrothermally in a two-stage process at $P(H_2O)$ = 2 kbar. A gel starting material was first crystallized at 375°C for one week. If the synthetic lizardite contained fewer than 0.5% impurities, it was hydrothermally treated for an additional one or two weeks at 385–390°C. Synthetic lizardite typically crystallized in aggregates of very fine-grained (0.006 mm) plates. Transmission electron-microscopy revealed that the synthetic product contained trace amounts of chrysotile. Unit-cell parameters of synthetic lizardite (Table 1) agree well with those reported by Chernosky (1975).

Clinochlore $Mg_5Al_2Si_3O_{10}(OH)_8$ was synthesized hydrothermally from a gel starting material at 650°C, $P(H_2O)$ = 3 kbar in 21 days. Synthetic clinochlore, which crystallizes in aggregates of fine-grained (0.03 mm) subhedral plates, was found to be the II*b*-layer type as defined by Brown & Bailey (1962); the synthetic product contained less than 0.5% impurities. The powder pattern and unit-cell parameters (Table 1) agree well with those determined for synthetic clinochlore (Chernosky 1974) and with those of an almost iron-free

TABLE 1. UNIT-CELL PARAMETERS AND VOLUMES OF SYNTHETIC TALC, FORSTERITE, CLINOCHLORE AND LIZARDITE

	talc	forsterite	clinochlore	lizardite
a	5.293(5)Å	4.751(1)Å	5.326(1)Å	5.316(6)Å
b	9.175(6)	10.198(1)	3.223(1)	9.229(10)
c	18.984(12)	5.979(1)	14.413(2)	7.254(14)
V	908.41 (71)	289.76 (5)	702.61 (20)	355.94 (82)
β	99°53'	--	--	--
N	14	42	21	13

Figures in parentheses represent the estimated standard deviation in terms of least units cited for the value to their immediate left; the uncertainties were calculated using a unit-cell refinement program and represent precision only. Abbreviations: N = number of reflections used in the unit-cell refinements.

natural chlorite from Cobargo, New South Wales (Loughnan & See 1958).

Forsterite Mg_2SiO_4 was synthesized hydrothermally at 800°C, $P(H_2O) = 0.7$ kbar in seven days. Crystals are fine grained (0.009 mm) and anhedral, with less than 0.5% impurities. The position of the (130) reflection at $d = 2.765$ coincides with d_{130} of synthetic forsterite (Fisher & Medaris 1969). The unit-cell parameters are presented in Table 1.

Talc $Mg_3Si_4O_{10}(OH)_2$ was synthesized hydrothermally at 680°C, $P(H_2O) = 2$ kbar in eight to ten days from an oxide mix. The product typically crystallized as aggregates of fine-grained (0.012 mm) plates with relatively low birefringence; the crystals contain less than 1% enstatite as an impurity, which may reflect a slight deficiency of silica in the starting material. The powder pattern and unit-cell parameters (Table 1) agree well with natural (PDF 13–558) and synthetic (Forbes 1971) talc.

The reaction $L = C + T + F + H_2O$

Two observations suggest that the upper thermal stability of lizardite is governed by the reaction $L_{ss} = C_{ss} + T_{ss} + F + H_2O$, where the subscript *ss* indicates that the phase subscripted is a crystalline solution: (1) the reaction occurs in metamorphosed serpentinites (Frost 1973, 1975) and (2) high-temperature synthesis experiments performed using lizardite bulk compositions ranging from $x = 0.2$ to 1.5 yield the assemblage chlorite + talc + forsterite.

The thermal stability of lizardite with $x = 0.5$ was determined by reversing the reaction

$$\underset{\text{lizardite}}{10Mg_{5.5}AlSi_{3.5}O_{10}(OH)_8} = \underset{\text{clinochlore}}{5Mg_5Al_2Si_3O_{10}(OH)_8} + \underset{\text{talc}}{2Mg_3Si_4O_{10}(OH)_2} + \underset{\text{forsterite}}{12Mg_2SiO_4} + 18H_2O.$$

This reaction is univariant provided that the composition of each phase remains constant over the P–T range investigated experimentally, and that each phase is in internal homogeneous equilibrium. Although it is extremely unlikely that the former condition was fulfilled, our data indicate that the compositions of the phases remained *nearly* constant.

Lizardite is a crystalline solution that decomposes over a range of temperatures at a given $P(H_2O)$. For a given pressure, only that lizardite (whose composition changes as a function of pressure) which persists to the highest temperature can be thought of as potentially stable in a thermodynamic sense. We emphasize the phrase "potentially stable in a thermodynamic sense" because the thermally most stable lizardite may have a higher Gibbs free energy and hence be metastable with respect to another assemblage such as chlorite + antigorite. The composition of the thermally most "stable" lizardite has not been determined; however, theoretical considerations (to be discussed later) suggest that it is near $x = 0.6$. In the light of the above discussion, the curve reversed during the course of this study is metastable; however, it provides useful information on lizardite stability and allows one to calculate the thermodynamic constants of lizardite.

Critical experiments that bracket the position of the reaction $L = C + F + T + H_2O$ in P–T space are shown in Table 2 and plotted on Figure 1. The brackets depicted in Figure 1 are fairly broad, because sluggish reaction rates near the phase boundary prevented tighter bracketing in a reasonable time. A mechanical mixture of Al-free talc, clinochlore ($x = 1.0$), forsterite and lizardite ($x = 0.5$) was used as starting material. Clinochlore and Al-free talc were used in the starting material because synthesis experiments using the $x = 0.5$ gel at a temperature above the stability of lizardite yielded these phases. In addition, the positions of key X-ray reflections on a powder pattern of the mechanically mixed starting material compare well with the positions on a powder pattern of the high-temperature as-

TABLE 2. EXPERIMENTS BRACKETING THE REACTION $10L = 5C + 2T + 12F + 18H_2O$

Experiment number	T (°C)	P_{H_2O} (kbars)	Duration (hours)	Comments	Extent of reaction
34	513(3)	0.5	2112	L(+)C(-)T(-)F(-)	M
42	553(4.5)	0.5	2376	L(-)C(+)T(+)F(+)	M
32	614(4)	0.5	1872	L(-)C(+)T(+)F(+)	M
41	546(3)	2.0	2400	L(+)C(-)T(-)F(-)	M
40	575(4)	2.0	2064	L(+)C(-)T(-)F(-)	S
39	607(1.5)	2.0	2400	L(-)C(+)T(+)F(+)	M
14	502(4)	3.0	3768	L(+)C(-)T(-)F(-)	S
16	536(1.5)	3.0	3456	L(+)C(-)T(-)F(-)	M
12	558(2)	3.0	1560	L(+)C(-)T(-)F(-)	W
35	568(6)	3.0	1248	L(+)C(-)T(-)F(-)	S
31	596(3)	3.0	2424	L(-)C(+)T(+)F(+)	S
10	518(4)	4.0	3264	L(+)C(-)T(-)F(-)	S
20	560(4.5)	4.0	3504	L(+)C(-)T(-)F(-)	M
30	573(2.5)	4.0	2544	L(+)C(-)T(-)F(-)	M
37	586(4.5)	5.0	2424	L(+)C(-)T(-)F(-)	M
36	615(3)	5.0	2424	L(-)C(+)T(+)F(+)	W
26	507(4)	6.0	4248	L(+)C(-)T(-)F(-)	S
3	533(3.5)	6.0	3360	L(+)C(-)T(-)F(-)	S
4	591(3)	6.0	888	L(+)C(-)T(-)F(-)	W
29	625(2.5)	6.0	1992	L(-)C(+)T(+)F(+)	W
28	678(3.5)	6.0	2472	L(-)C(+)T(+)F(+)	S

Growth of diminution of a phase is indicated by a (+) or (-) respectively. All assemblages include water. Parenthesized numbers represent two standard deviations from the calculated mean temperatures to their immediate left. Symbols S, M, and W are qualitative estimates of the extent of reaction and represent greater than 75 percent, 75 to 50 percent, and less than 50 percent, respectively.

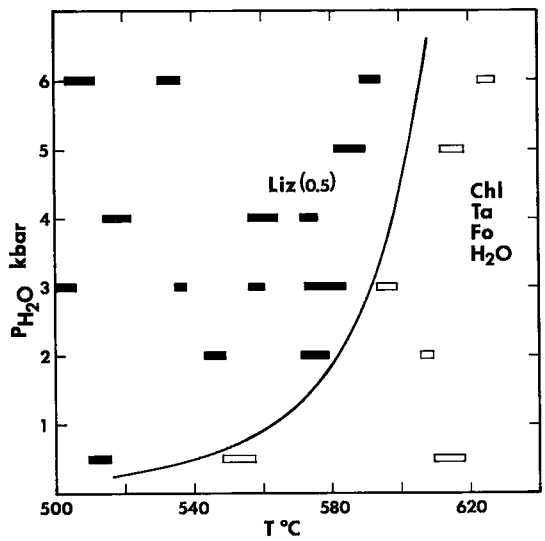

FIG. 1. Dehydration curve for the reaction 10L = 5C + 2T + 12F + $18H_2O$. Solid symbols represent growth of lizardite; open symbols represent growth of high-temperature assemblage. Size of symbols represents uncertainty in measurement of temperature and pressure.

semblage crystallized using the $x = 0.5$ gel. The powder patterns were recorded with a Guinier camera, which allows very small shifts in peak positions to be detected. Within the limits of measurement, basal reflections of chlorite and talc occurred at the same positions in both the mechanical mixture and the synthetic high-temperature assemblage.

We were unable to determine the compositions of chlorite, talc and lizardite in the majority of the reversal experiments. The fine grain-size and intimate intergrowth of these phases in the reversal experiments precluded analysis with an electron-probe microanalyzer. Although the basal spacings of chlorite, talc and lizardite are sensitive to aluminum content, the amount of new growth was generally too small to influence the position of key X-ray reflections. Attempts to increase the relative amount of new growth by using two starting materials (one containing 20% and the other 80% of lizardite by weight) for each reversal failed because of the small number of lizardite reflections, many of which are "masked" by chlorite reflections. Reversals could only be detected in the starting material containing 80% lizardite.

The positions of chlorite, lizardite and talc basal reflections in several reversals showing considerable reaction (Table 2, experiments 3, 10, 14, 26, 28, 31, 35 and 40) indicate that the compositions of these phases do not change significantly. These data suggest that the com-

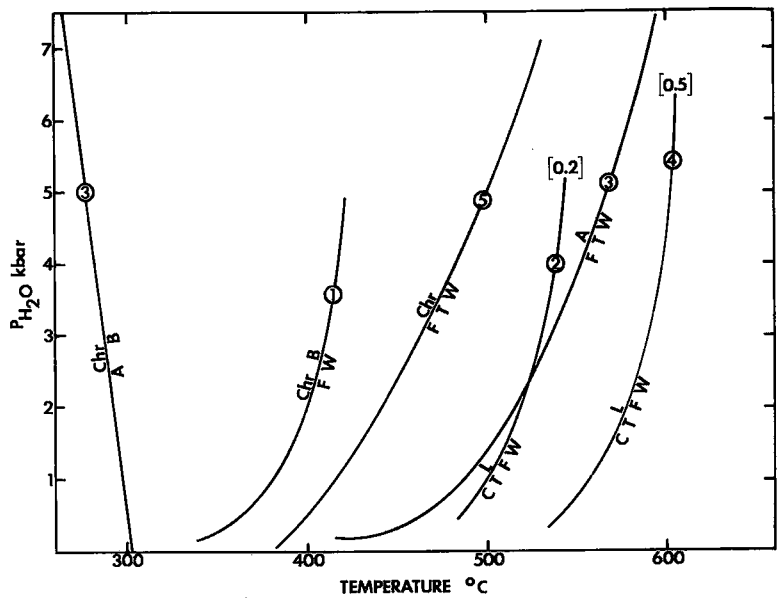

FIG. 2. P–T diagram illustrating relative stabilities of chrysotile, lizardite and antigorite. Numbers in circles refer to source of data: (1) Johannes (1968), (2) Chernosky (1973a), (3) Evans *et al.* (1976), (4) this study, (5) Chernosky (1973b).

positions of phases in those reversals showing little reaction also do not depart significantly from the compositions of phases used in the starting material. We suggest that exchange equilibrium was achieved, at least with respect to the rims of grains, and that the curve shown in Figure 1 closely approximates the dehydration boundary for lizardite with $x = 0.5$.

Although there was about 15% chrysotile in the low-temperature assemblage, the apparent thermal stability of lizardite with $x = 0.2$ (3.7 wt. % Al_2O_3) is 60°C lower at $P(H_2O) = 2$ kbar than the stability of lizardite with $x = 0.5$ (Fig. 2). Chernosky (1973a) was not able to synthesize $x = 0.2$ lizardite free of chrysotile impurity; growth of low-aluminum chrysotile from the $x = 0.2$ lizardite starting material forces the lizardite to more aluminous compositions. Unfortunately, Chernosky was not able to determine the compositions of the coexisting lizardite and chrysotile, nor was he able to determine whether chrysotile is an impurity or whether it actually belongs to the low-temperature assemblage. Although the curves for lizardite with $x = 0.2$ and $x = 0.5$ are not directly comparable, they clearly indicate that the decomposition temperature of lizardite increases with increasing aluminum content.

Discussion

Relative stabilities of serpentine minerals

Differences in the habit and stability (Fig. 2) of chrysotile, lizardite and antigorite arise because of the complex interplay between composition and the structural adjustments required to achieve articulation between the octahedral and tetrahedral sheets along a common plane. Compositional differences among the serpentine minerals are small (Page 1968, Whittaker & Wicks 1970) but important because they control the lateral dimensions of the octahedral and tetrahedral sheets.

Although iron is a ubiquitous component in natural serpentines, we shall evaluate serpentine stabilities in the light of the structure variations induced by the coupled substitution $2Al = Mg + Si$. Because iron possesses two valence states, its substitution in serpentine is more complex than the substitution of aluminum. Although the effect of iron on the lateral dimensions of the octahedral and tetrahedral sheets can be evaluated by considering the ionic radii of Fe^{2+} and Fe^{3+} relative to the ionic radius of Al^{3+}, we shall not do so in this discussion.

The abundance of chrysotile in dilation veins and the ease with which this phase is synthesized in the laboratory suggest that curling of the octahedral sheets is the preferred mechanism of misfit relief for the composition $x = 0$ at temperatures below about 300°C at $P(H_2O) = 2$ kbar, whereas partial curling accompanied by tetrahedral inversion, as in antigorite, is the preferred mechanism of misfit relief at temperatures between 300° and 500°C at $P(H_2O) = 2$ kbar. Lizardite with $x = 0$ has been synthesized (Jasmund & Sylla 1971, 1972, Chernosky 1973a, 1975), suggesting that the distortion accompanying the formation of a flat-layer serpentine may not be much more severe than the distortion accompanying curling (Wicks & Whittaker 1975).

Both lizardite and chrysotile crystallize if starting materials with $0 < x \leq 0.25$ (Nelson & Roy 1958, Gillery 1959) are used. Chernosky (1975) observed that chrysotile tubes coexisting with lizardite become shorter, thicker and less abundant as the aluminum content of the starting material is increased, and he suggested that chrysotile incorporates a minor amount of this component.

The coupled substitution $2Al = Mg + Si$ leads to stabilization of lizardite because it results in an expansion of the lateral dimensions of the tetrahedral sheet and a contraction of the lateral dimensions of the octahedral sheet. As the lateral dimensions of the two sheets become similar, the serpentine layer no longer curls but forms lizardite. As the structure of lizardite becomes more stable, its free energy decreases and soon becomes less than that of chrysotile. The rapid decrease in the free energy of lizardite is manifest in the dramatic rise in its thermal decomposition temperature. For example, the thermal decomposition temperature of lizardite with $x = 0.2$ is considerably higher than that of chrysotile and is about equivalent to that of antigorite (Fig. 2).

The widespread coexistence of chrysotile and lizardite in rocks can be rationalized by assuming that these serpentines form separate solid solutions. The addition of variable amounts of Fe^{2+} and Fe^{3+} as well as Al virtually ensures that both phases will coexist stably over a finite and perhaps rather wide temperature interval. Lizardites with compositions $x < 0.15$ are probably metastable with respect to antigorite at temperatures above 400°C at $P(H_2O) = 2$ kbar.

Continued substitution of Al for Si + Mg progressively decreases the free energy of lizardite relative to chrysotile; the chrysotile

structure is probably highly unstable if its aluminum content is greater than about $x = 0.10$. The structural stability (hence, thermal stability) of lizardite is expected to reach a maximum at the composition where the lateral dimensions of the octahedral and tetrahedral sheets are equivalent. Radoslovich (1963) calculated that b for both sheets will be identical at $x = 0.75$, whereas Chernosky (1975) calculated that the area of both sheets will be identical at $x = 0.6$. This limit will be raised if Fe^{2+} replaces Mg or if Fe^{3+} replaces octahedral Al, and lowered if Fe^{3+} replaces tetrahedral Al.

It is probably not coincidence that the compositional break between the one- and six-layer lizardite structures occurs at the point ($x = 0.6$) where the tetrahedral and octahedral sheets reach an equivalent size. Once the optimum aluminum content is exceeded, the dimensions of the tetrahedral sheet grow larger than the dimensions of the octahedral sheet. Articulation is achieved by decreasing the lateral dimensions of the tetrahedral sheet; the decrease is achieved by rotation of adjacent tetrahedra in opposite directions in the (001) plane (Radoslovich & Norrish 1962). The different surprising that Al-lizardite persists to higher is presumably more conducive to different stacking arrangements in the c direction.

The remarkable influence of aluminum on the thermal decomposition temperature of lizardite is illustrated in Figure 2. It is not surprising that Al-lizardite persists to higher temperatures than Al-free antigorite; the structural adjustments necessary to achieve articulation in antigorite are more severe than in those lizardites having aluminum contents ranging from $x = 0.25$ to about 0.6.

Assuming that lizardite and antigorite are members of two separate crystalline solutions, it is reasonable to expect that their stability fields overlap and that they might coexist stably under favorable circumstances. The range of lizardite compositions that can coexist with antigorite is probably extended by iron substitution in both minerals and by Al and Cr substitution in antigorite. The assumption that lizardite and antigorite form separate solid solutions is supported by structural data indicating that these serpentines are not polymorphs (Wicks & Whittaker 1975) and by analytical data indicating that antigorites have higher SiO_2 and lower MgO and H_2O^+ contents than ideal serpentine, whereas lizardites have MgO and SiO_2 contents close to those of ideal serpentine but H_2O^+ contents that are higher (Whittaker & Wicks 1970).

In the light of the above discussion, it is surprising that lizardites with aluminum contents between $x = 0.31$ (5.7 wt. % Al_2O_3) (Frost 1975) and $x \approx 0.6$–0.7 have not been reported. Solely on theoretical grounds, one would predict that lizardites with aluminum contents in this range should exist. Several explanations might account for the discrepancy between theory and observation: (1) aluminous lizardites in this range exist but have not been discovered, (2) substitution of other cations such as Cr, Fe^{2+} and Fe^{3+} favors a structure of lower aluminum content, and (3) the assemblage chlorite + antigorite, which is chemically equivalent to lizardite, is stable with respect to lizardite.

Lizardites with aluminum contents higher than $x = 0.7$ have been reported; however, they are multilayer types which will not be discussed here.

Thermodynamic calculations

Gordon's (1973) technique has been used to obtain the range of permissible $\Delta G°_r$ and $\Delta S°_f$ values that together satisfy a set of linear inequalities of the form $\Delta G°_r \lesssim 0$, where $\Delta G°_r = (T\text{–}298)\Delta S°_{f,s} + (P\text{–}1)\Delta V_s + G*_{H_2O}$.

Each linear inequality of the set was obtained from an experimental reversal of L = F + T + C + H_2O (Table 2); the left-hand side of the inequality is greater than zero if the reactants are stable, and less than zero if the products are stable. The lack of heat capacity, thermal expansivity and compressibility data for all the solid phases requires the assumption that $\Delta S°_{f,s}$ and ΔV_s are constants independent of P and T; Zen (1969) showed that the uncertainties introduced by making these assumptions are small. An added assumption is that the compositions of all the phases remain constant along the "univariant" curve. As shown earlier, the compositions of the phases probably do not differ significantly along the curve. The shaded region in Figure 3 contains all the $\Delta G°_r$, $\Delta S°_{f,s}$ pairs consistent with three critical experiments (Table 2, experiments 36, 40 and 42). The remaining experiments are consistent with Figure 3 but do not provide additional constraints. The range of permissible $\Delta S°_{f,s}$ values that satisfy the inequalities is 214.3 to 310.7 J mol^{-1} deg^{-1}; the range of permissible $\Delta G°_r$ values is 273.4 to 324.3 kJ mol^{-1}.

Knowledge of $\Delta G°_r$ and $\Delta S°_{f,s}$ will allow us to calculate the free energy and entropy of

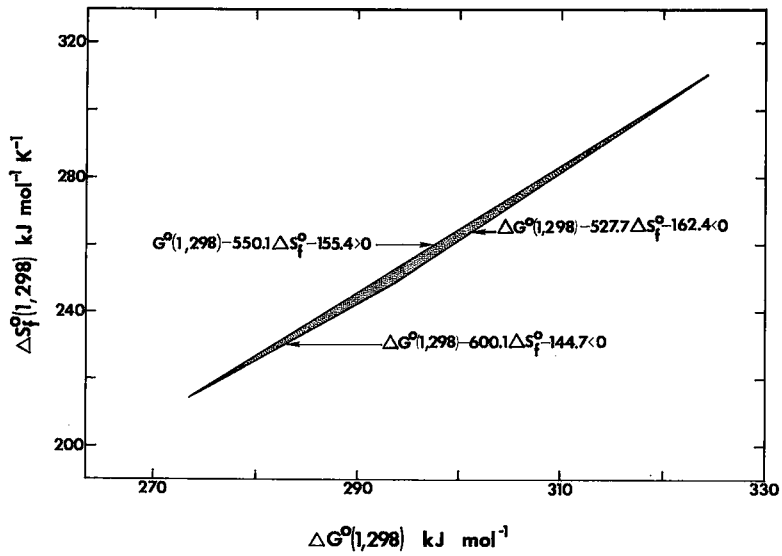

FIG. 3. Standard-state free energy *versus* standard-state entropy diagram showing three inequalities corresponding to experiments 36, 40 and 42 (Table 2). Shaded portion contains values satisfying all three inequalities simultaneously.

TABLE 3. THERMODYNAMIC PARAMETERS OF PHASES

	$\Delta G^{\circ}_{f}(1, 298)$ kJ mol^{-1}	$\Delta H^{\circ}_{f}(1, 298)$ kJ mol^{-1}	$\Delta S^{\circ}_{f}(1, 298)$ J mol^{-1}deg^{-1}	V(1, 298) J bar^{-1} gf^{-1}
Lizardite	-8220.05 ± 47.60(3)	-8902.77 ± 54.13(3)	-2289.86 ± 86.47(3)	21.255 ± 0.048(3)
Clinochlore	-8231.27 ± 8.37(7)	-8877.45 ± 9.17(7)	-2167.31 ± 12.55(4)	21.159 ± 0.006(3)
Talc	-5513.69 ± 4.69(6)	-5893.26 ± 4.72(6)	-1273.08 ± 0.08(5)	13.625 ± 0.026(1)
Forsterite	-2051.70 ± 1.90(8)	-2170.66 ± 1.91(6)	-398.88 ± 0.88(5)	4.379 ± 0.003(1)
Brucite			-305.18 ± 0.19(1)	2,463 ± 0.007(1)
Antigorite			-17738.99 ± 29.48(2)	174.910 ± 0.860(2)

Numbers in parentheses refer to source of data: (1) Robie et al. 1978; (2) Evans et al. 1976; (3) This study; (4) Zen & Chernosky 1976; (5) Zen 1972; (6) Chernosky & Autio 1979; (7) Chernosky 1974; (8) Hemingway & Robie, unpublished.

formation of lizardite provided the free energies and entropies of clinochlore, forsterite and talc are known. Unfortunately, the free energy of talc is a matter of current debate (Bricker *et al.* 1973, Zen & Chernosky 1976, Hemley *et al.* 1977, Robie *et al.* 1978). Although the free energy of clinochlore has been calculated by Chernosky (1974), it is subject to considerable uncertainty (compare with Helgeson *et al.* 1978 and Newton & Wood 1979).

Using –5513.69 ± 4.69 kJ mol^{-1} for ΔG°_{f}, talc and –8231.27 ± 8.37 kJ mol^{-1} for ΔG°_{f}, clinochlore, together with the thermochemical values in Table 3 and values of Fisher & Zen (1971) for $G^{*}(H_2O)$, we obtain values for $\Delta S^{\circ}_{f}(L) = -2290 \pm 86$ J mol^{-1} deg^{-1} and $\Delta G^{\circ}_{f}(L) = -8220 \pm 48$ kJ mol^{-1}. Using these entropy and free-energy values we obtain –8903 ± 54 kJ mol^{-1} for ΔH°_{f} of lizardite. The large errors attached to the entropy and free energy of lizardite are a consequence of sluggish reaction rates, which make it difficult to bracket the reaction more tightly. The reader can modify the thermochemical parameters for lizardite as refined values for talc and clinochlore become available.

Uncertainties attached to the thermodynamic parameters of lizardite were obtained by combining the uncertainties in the temperature and pressure of each experiment with the uncertainties in the entropies, molar volumes and free energies of talc, chlorite, forsterite and H_2O, and in the molar volume of lizardite. Uncertainties in the ancillary thermochemical data (Table 3) were calculated by summing the uncertainties for each phase. Uncertainty in the measurement of pressure is assumed to be 1 %. Temperature uncertainty was accounted for by using those points on the error bars most distant from the equilibrium curve rather than the mean temperature of the error bars.

Lizardite–antigorite phase relations and petrological implications

The mutual phase relations among antigorite and Al-lizardite are poorly understood. In order to explore lizardite–antigorite phase relations in detail, a multisystem (Fig. 4) involving clinochlore, antigorite, lizardite ($x = 0.5$), brucite, talc, forsterite and H_2O in the system MgO–Al_2O_3–SiO_2–H_2O was constructed. Chrysotile is not included in the analysis because we are primarily concerned with reactions occurring at temperatures above its stability. Owing to compositional degeneracy, only ten univariant reactions (Table 4) relate the six univariant points shown in Figure 4. Compatibility relations for the divariant fields shown in Figure 4 are given in Figure 5.

Two possible version of the closed net are depicted in Figure 4; both versions are constructed in such a manner that H_2O generally appears on the high-temperature, low-pressure side of each reaction. Experimental data (Fig. 2) indicate that reaction L = F + C + T + H_2O occurs at higher temperatures than the reaction A = F + T + H_2O for pressures below [B] and that the stability of lizardite

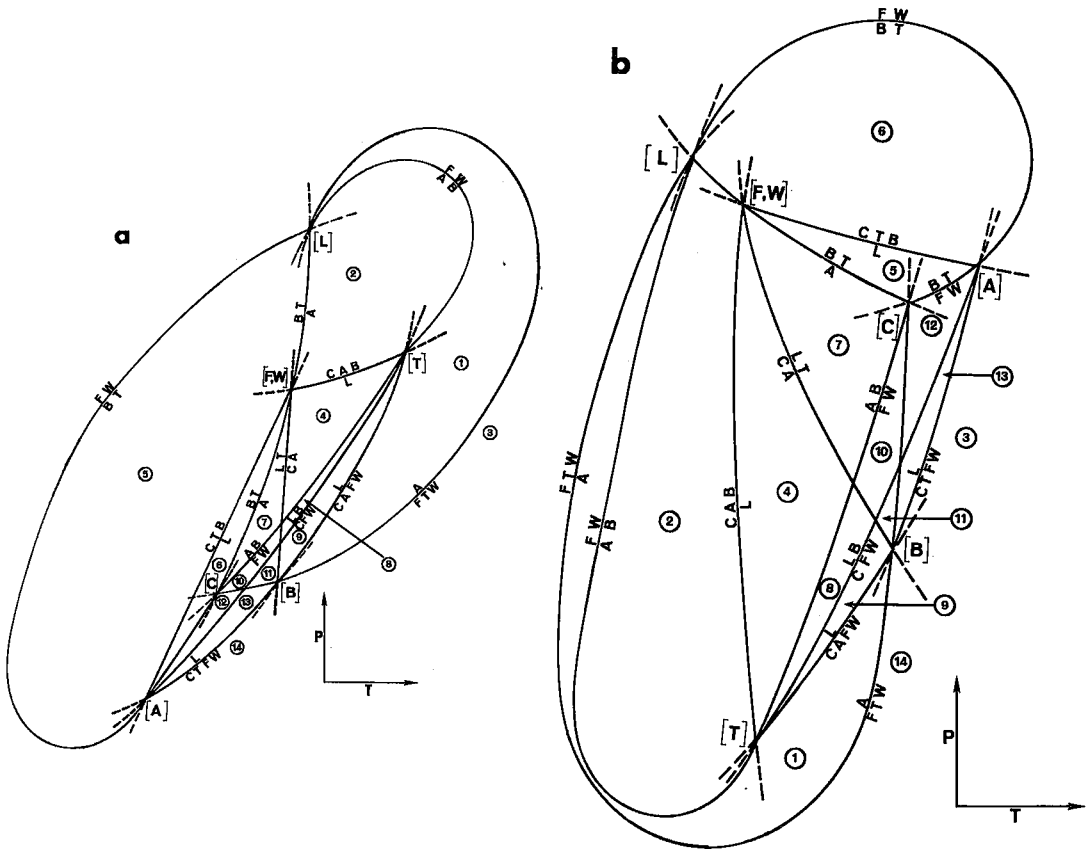

FIGS. 4a and b. Two possible closed nets for the MgO–Al_2O_3–SiO_2–H_2O multisystem involving the phases lizardite, antigorite, clinochlore, talc, forsterite, brucite and vapor. Compatibility diagrams for each numbered divariant field are given in Figure 5.

TABLE 4. BALANCED UNIVARIANT REACTIONS IN THE LIZARDITE-ANTIGORITE MULTISYSTEM

Reactions	Absent phases
(1) 10L = 5C + 2T + 12F + $18H_2O$	(AB)
(2) A = 18F + 4T + $27H_2O$	(CLB)
(3) 20L = 10C + A + 6F + $9H_2O$	(BT)
(4) 2L + 2B = 4F + C + $6H_2O$	(AT)
(5) A + 20B = 34F + $51H_2O$	(CLT)
(6) T + 5B = 4F + $6H_2O$	(CLA)
(7) 17T + 45B = 2A	(CLFW)
(8) 2L = C + T + 3B	(AFW)
(9) 34L = 17C + 2A + 6B	(FTW)
(10) 30L + 2T = 2A + 15C	(BFW)

increases with increasing aluminum content. These features are consistent only with Figure 4a.

Having established the correct orientation for the multisystem, one can readily compare assemblages and sequences of reactions observed in nature with those predicted by the been recrystallized at fluid pressures on the multisystem (Fig. 5) in order to establish which portions of the multisystem might be applicable to rocks. Figure 4a is consistent with the following sequence of divariant assemblages found in progressive metamorphism: A + B (Rost 1949, Dietrich & Peters 1971, Coleman 1971, Trommsdorff & Evans 1974), A + F (Evans *et al.* 1976), C + A (Frost 1975, Evans 1977), and F + T (Trommsdorff & Evans 1974, Frost 1975, Coleman 1971). Figure 4a is also consistent with the following reactions found in progressive metamorphism (Evans *et al.* 1976): A + B = F + H_2O and A = F + T + H_2O.

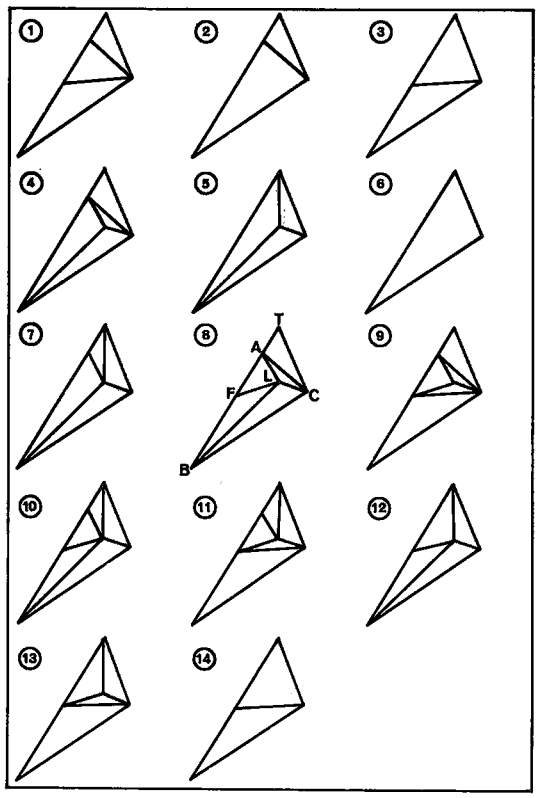

FIG. 5. Compatibility diagrams for the numbered divariant fields in Figures 4a and b.

On the strength of the observation that the pair antigorite + chlorite occurs widely in thoroughly recrystallized serpentinites, Evans (1977, p. 410) suggested that "lizardite probably occurs stably, if at all, only at very low temperatures." However, Frost (1973) observed that lizardite veins persist in a contact aureole 30 metres beyond the antigorite-out isograd, and he considered the possibility that lizardite is stable relative to antigorite. More recently, Frost (1975) has suggested that lizardite is metastable on the basis of Evans's observation that the chemically equivalent pair antigorite + chlorite is the stable assemblage in the Alps.

Metaserpentinites in the Sultan–Darrington area contain Al–lizardite bastites in a matrix of mesh serpentine recrystallized to Al- and Cr-poor antigorite (Dungan 1977). Dungan was not able to determine whether the association of Al–lizardite with antigorite represents stable coexistence of two serpentine phases or metastable persistence of the lizardite bastites relative to more stable antigorite.

The conflicting opinions regarding the stability of antigorite relative to lizardite are not yet resolved. According to the multisystem shown in Figure 4a, antigorite should persist to higher temperatures than lizardite at pressures above [B], whereas at pressures below [B] lizardite should persist to higher temperatures than Al-free antigorite. This is consistent with phase relations in metaserpentinites from Paddy-Go-Easy Pass described by Frost (1973, 1975). Interpolation between the $x = 0.2$ and $x = 0.5$ lizardite dehydration curves on Figure 6 suggests that invariant point [B] will occur near water pressures of 3 kbar; *i.e.*, lizardite should be stable below this pressure. This is consistent with Frost's (1975) estimate that the rocks at Paddy-Go-Easy Pass recrystallized at pressures below 3 kbar. Many regionally metamorphosed

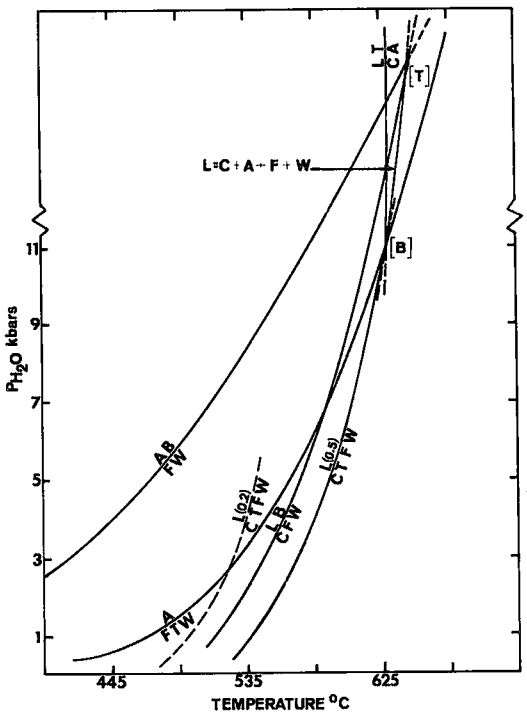

FIG. 6. Refined version of multisystem shown in Figure 4a. The reactions A = F + T + W and L = C + T + F + W have been located experimentally. The positions of the reactions A + B = F + W, L + B = C + F + W and L + T = C + A are constrained by the topology around the talc-absent and brucite-absent invariant points (Fig. 4a).

ultramafic rocks in the Italian Alps which contain the assemblage chlorite + antigorite have order of 7 kbar (Evans, pers. comm.), which is consistent with Figure 4a. However, this assemblage is also found in progressively metamorphosed serpentinite in the Bergell aureole, where fluid pressure probably did not exceed 2 kbar (Trommsdorff & Evans 1972). Although this observation is inconsistent with Figure 4a, it should be noted that antigorites coexisting with chlorite in the Bergell aureole contain from 1.1 to 2.7 wt. % Al_2O_3 and about 0.25 wt. % Cr_2O_3 (Trommsdorff & Evans 1972, Table 4). The addition of Al_2O_3 to antigorite probably expands its stability field and drives the reaction A = F + T + W (Fig. 6) toward higher temperatures, thereby expanding the stability field of antigorite + chlorite. The assumption that the addition of Al_2O_3 stabilizes antigorite is reasonable. Substitution of Al_2O_3 into both the octahedral and tetrahedral sheets presumably decreases the mismatch between the sheets and tends to flatten them out, thereby decreasing intralayer strain and increasing structural stability.

The phase relations depicted in Figure 4a indicate that Al–lizardite and antigorite can coexist in rocks having an appropriate bulk composition. An additional reaction, L + B = C + F + H_2O, is predicted to occur at higher temperature than A + B = F + H_2O at all water pressures. Although the assemblage L + B is very common, the reaction L + B = C + F + H_2O has not been recognized in metamorphosed serpentinites.

The compatibility relations observed in rocks can be used to determine the portion of Figure 4a that might pertain to nature. The assemblage B + T has not been observed, suggesting that phase relations on the low-temperature side of the reaction B + T = A can be neglected. Hence [B] and perhaps [T] are the only invariant points which are likely to be relevant to rocks. If the experimental work on antigorite (Evans *et al.* 1976) and lizardite (current study) is used as a constraint, Figure 4a can be "opened up" (Fig. 6). The position of the reaction A + B = F + H_2O was calculated by Evans *et al.* (1976). The position of the reaction L + B = C + F + H_2O has not been calculated, but it is constrained to lie between the reactions A + B = F + H_2O and L = C + T + F + H_2O. Location of the indifferent crossing between A = F + T + H_2O and L + B = C + F + H_2O has not been determined, but probably occurs at very low pressure for lizardites containing less than 5 wt. % Al_2O_3.

In summary, we suggest that Al–lizardite may be stable with respect to chlorite + low-Al antigorite in serpentinites recrystallized at low pressures. Although Figure 6 seems consistent with phase relations determined experimentally and with those observed in some recrystallized serpentinites, the model needs considerable testing in the field.

The P–T coordinates for equilibria shown in Figure 6 should be applied to rocks with caution. The experiments were performed at $P(H_2O) = P_{total}$. Natural fluids are not pure H_2O; hence P_{fluid} is not equal to P_{total}. The unknown effects of Fe^{2+}, Fe^{3+} and chromium on the stability fields of lizardite and antigorite and of Al on that of antigorite may change the phase relations depicted in Figures 4a and 6.

ACKNOWLEDGEMENTS

This research was supported by NSF grant EAR74–1339A01 to J.V. Chernosky, Jr. Discussions of lizardite phase-relations with M. A.

Dungan, B.W. Evans, B.R. Frost, P.H. Osberg and F.J. Wicks were stimulating and contributed to the ideas expressed in the paper.

References

APPLEMAN, D.E. & EVANS, H.T., JR. (1973): Job 9214: Indexing and least-squares refinement of powder diffraction data. *Nat. Tech. Inf. Serv.*, U.S. Dept. Comm., Springfield, Va., PB 216 188.

BAILEY, S.W. (1969): Polytypism of trioctahedral 1:1 layer silicates. *Clays Clay Minerals* **17**, 355-371.

BRICKER, O.P., NESBITT, H.W. & GUNTER, W.D. (1973): The stability of talc. *Amer. Mineral.* **58**, 64-72.

BROWN, B.E. & BAILEY, S.W. (1962): Chlorite polytypism. I. Regular and semirandom one-layer structures. *Amer. Mineral.* **47**, 819-850.

BURNHAM, C.W., HOLLOWAY, J.R. & DAVIS, N.F. (1969): Thermodynamic properties of water to 1000°C and 10,000 bars. *Geol. Soc. Amer. Spec. Pap.* **132**.

CHERNOSKY, J.V., JR. (1973a): *An Experimental Investigation of the Serpentine and Chlorite Group Minerals in the System MgO–Al_2O_3–SiO_2–H_2O.* Ph.D. thesis, Mass. Inst. Tech., Cambridge, Mass.

——— (1973b): The stability of chrysotile, $Mg_3Si_2O_5(OH)_4$, and the free energy of formation of talc, $Mg_3Si_4O_{10}(OH)_2$. *Geol. Soc. Amer. Program Abstr.* **5**, 575.

——— (1974): The upper stability of clinochlore at low pressure and the free energy of formation of Mg–cordierite. *Amer. Mineral.* **59**, 496-507.

——— (1975): Aggregate refractive indices and unit cell parameters of synthetic serpentine in the system MgO–Al_2O_3–SiO_2–H_2O. *Amer. Mineral.* **60**, 200-208.

——— & AUTIO, L.K. (1979): The stability of anthophyllite in the presence of quartz. *Amer. Mineral.* **64**, 294-303.

COLEMAN, R.G. (1971): Petrologic and geophysical nature of serpentinites. *Geol. Soc. Amer. Bull.* **82**, 897-918.

DIETRICH, V. & PETERS, T. (1971): Regionale Verteilung der Mg–Phyllosilikate in den Serpentiniten des Oberhalbsteins. *Schweiz. Mineral. Petrog. Mitt.* **51**, 329-348.

DUNGAN, M.A. (1977): Metastability in serpentine–olivine equilibria. *Amer. Mineral.* **62**, 1018-1029.

——— (1979): A microprobe study of antigorite and some serpentine pseudomorphs. *Can. Mineral.* **17**, 771-784.

EVANS B.W. (1977): Metamorphism of alpine peridotite and serpentinite. *Ann. Rev. Earth Planet. Sci.* **5**, 397-447.

———, JOHANNES, W., OTERDOOM, H. & TROMMSDORFF, V. (1976): Stability of chrysotile and antigorite in the serpentinite multisystem. *Schweiz. Mineral. Petrog. Mitt.* **56**, 79-93.

FISHER, G.W. & MEDARIS, L.G., JR. (1969): Cell dimensions and X-ray determinative curve for synthetic Mg–Fe olivines. *Amer. Mineral.* **54**, 741-753.

FISHER, J.R. & ZEN, E-AN (1971): Thermodynamic calculations from hydrothermal phase equilibrium data and the free energy of H_2O. *Amer. J. Sci.* **270**, 297-314.

FORBES, W.C. (1971): Iron content of talc in the system $Mg_3Si_4O_{10}(OH)_2$–$Fe_3Si_4O_{10}(OH)_2$. *J. Geol.* **79**, 63-74.

FROST, B.R. (1973): *Contact Metamorphism of the Ingalls Ultramafic Complex at Paddy-Go-Easy Pass, Central Cascades, Washington.* Ph.D. thesis, Univ. Washington, Seattle, Wash.

——— (1975): Contact metamorphism of serpentinite, chloritic blackwall and rodingite at Paddy-Go-Easy Pass, Central Cascades, Washington. *J. Petrology* **16**, 272-313.

GILLERY, F.H. (1959): The X-ray study of synthetic Mg–Al serpentines and chlorites. *Amer. Mineral.* **44**, 143-152.

GORDON, T.M. (1973): Determination of internally consistent thermodynamic data from phase equilibrium experiments. *J. Geol.* **81**, 199-208.

HELGESON, H.C., DELANY, J.M., NESBITT, H.W. & BIRD, D.K. (1978): Summary and critique of the thermodynamic properties of rock-forming minerals. *Amer. J. Sci.* **278-A**, 1-229.

HEMLEY, J.J., MONTOYA, J.W., CHRIST, C.L. & HOSTETLER, P.B. (1977): Mineral equilibria in the MgO–SiO_2–H_2O system. I. Talc–chrysotile–forsterite–brucite stability relations. *Amer. J. Sci.* **277**, 322-351.

JASMUND, K. & SYLLA, H.M. (1971): Synthesis of Mg- and Ni-antigorite. *Contr. Mineral. Petrology* **34**, 84-86.

——— & ——— (1972): Synthesis of Mg- and Ni-antigorite: A correction. *Contr. Mineral. Petrology* **34**, 346.

JOHANNES, W. (1968): Experimental investigation of the reaction forsterite + H_2O ⇌ serpentine + brucite. *Contr. Mineral. Petrology* **19**, 309-315.

LOUGHNAN, F.C. & SEE, G.T. (1958): A white chlorite from Cobargo, New South Wales. *Amer. Mineral.* **43**, 671-676.

NELSON, B.W. & ROY, R. (1958): Synthesis of the chlorites and their structural and chemical constitution. *Amer. Mineral.* **43**, 707-725.

NEWTON, R.C. & WOOD, B.J. (1979): Thermodynamics of water in cordierite and some petrologic consequences of cordierite as a hydrous phase. *Contr. Mineral. Petrology* **68**, 391-405.

PAGE, N.J (1968): Chemical differences among the serpentine "polymorphs". *Amer. Mineral.* **53**, 201-215.

RADOSLOVICH, E.W. (1963): The cell dimensions and symmetry of layer lattice silicates. VI. Serpentine and kaolin morphology. *Amer. Mineral.* **48**, 368-378.

——— & NORRISH, K. (1962): The cell dimensions and symmetry of layer lattice silicates. I. Some structural considerations. *Amer. Mineral.* **47**, 599-616.

ROBIE, R.A., BETHKE, P.M., TOULMIN, M.S. & EDWARDS, J.L. (1966): X-ray crystallographic data, densities, and molar volumes of minerals. *Geol. Soc. Amer. Mem.* **97**, 27-73.

———, HEMINGWAY, B.S. & FISHER, J.R. (1978): Thermodynamic properties of minerals and related substances at 298.15 K and 1 bar (10^5 Pascals) pressure and at higher temperatures. *U.S. Geol. Surv. Bull.* **1452**.

ROST, F. (1949): Das Serpentinit–Gabbro–Vorkommen von Wurlitz und seine Mineralien. *Heidelberg. Beitr. Mineral. Petrog.* **1**, 626-688.

ROY, D.M. & ROY, R. (1955): Synthesis and stability of minerals in the system MgO–Al_2O_3–SiO_2–H_2O. *Amer. Mineral.* **40**, 147-178.

RUCKLIDGE, J.C. & ZUSSMAN, J. (1965): The crystal structure of the serpentine mineral, lizardite $Mg_3Si_2O_5(OH)_4$. *Acta Cryst.* **19**, 381-389.

TROMMSDORFF, V. & EVANS, B.W. (1972): Progressive metamorphism of antigorite schist in the Bergell tonalite aureole (Italy). *Amer. J. Sci.* **272**, 423-437.

——— & ——— (1974): Alpine metamorphism of peridotitic rocks. *Schweiz. Mineral. Petrog. Mitt.* **54**, 333-352.

WHITTAKER, E.J.W. & WICKS, F.J. (1970): Chemical differences among the serpentine "polymorphs': a discussion. *Amer. Mineral.* **55**, 1025-1047.

——— & ZUSSMAN, J. (1956): The characterization of serpentine minerals by X-ray diffraction. *Mineral. Mag.* **31**, 107-126.

WICKS, F.J. & PLANT, A.G. (1979): Electron-microprobe and X-ray-microbeam studies of serpentine textures. *Can. Mineral.* **17**, 785-830.

——— & WHITTAKER, E.J.W. (1975): A reappraisal of the structures of the serpentine minerals. *Can. Mineral.* **13**, 227-243.

YODER, H.S., JR. (1952): The MgO–Al_2O_3–SiO_2–H_2O system and related metamorphic facies. *Amer. J. Sci. Bowen Vol.*, 569-627.

ZEN, E-AN (1969): Free energy of formation of pyrophyllite from hydrothermal data: values, discrepancies and implications. *Amer. Mineral.* **54**, 1592-1606.

——— (1972): Gibbs free energy, enthalpy and entropy of ten rock-forming minerals: calculations, discrepancies, implications. *Amer. Mineral.* **57**, 524-553.

——— & CHERNOSKY, J.V., JR. (1976): Correlated free energy values of anthophyllite, brucite, clinochrysotile, enstatite, forsterite, quartz and talc. *Amer. Mineral.* **61**, 1156-1166.

APPENDIX: SYMBOLS AND NOTATION

A	antigorite $Mg_{48}Si_{34}O_{85}(OH)_{62}$
B	brucite $Mg(OH)_2$
Chr	chrysotile $Mg_3Si_2O_5(OH)_4$
C	clinochlore $Mg_5Al_2Si_3O_{10}(OH)_8$
F	forsterite Mg_2SiO_4
L	lizardite $Mg_{5.5}Al_{1.0}Si_{3.5}O_{10}(OH)_8$
T	talc $Mg_3Si_4O_{10}(OH)_2$
W	H_2O
$\Delta G°_f$	standard Gibbs free energy of formation (298.15 K, 1 bar) of a phase from the elements, in kJ mol^{-1}
$\Delta G°_r$	Gibbs free energy of reaction at 1 bar and 298.15 K
G^*	Gibbs free energy of H_2O at T and P according to data of Burnham *et al.* (1969), consistent with the standard state at 298.15 K and 1 bar
$\Delta H°_f$	standard enthalpy of formation (298.15 K, 1 bar) of a phase from the elements, in kJ mol^{-1}
$\Delta H°_r$	standard enthalpy of reaction at 1 bar and 298.15 K
V	volume of an individual phase, in J bar^{-1}
ΔV_s	volume change of the solid phases for a given reaction
$\Delta S°_f$	standard entropy of formation (298.15 K, 1 bar) of a phase from the elements, in J mol^{-1} deg^{-1}
$\Delta S°_{f,s}$	change of the entropy of formation of the solid phases for a given reaction at 1 bar and 298.15K

1 thermochemical calorie = 4.1840 joules

Received June 1979, revised manuscript accepted September 1979.